



# Heat transfer and friction characteristics of plain fin-and-tube heat exchangers, part I: new experimental data

Chi-Chuan Wang\*, Kuan-Yu Chi

*Energy and Resources Laboratories, Industrial Technology Research Institute, Hsinchu, Taiwan*

Received 5 November 1998; received in revised form 19 October 1999

## Abstract

This study presents the airside performance of fin-and-tube heat exchangers with plain fin configurations. A total of 18 samples were tested. The effect of the number of tube rows, fin pitch and tube diameter on the thermal-hydraulic characteristics was examined. Depending on the number of tube rows, it was found that the heat transfer characteristics were strongly related to the fin pitch. For  $N = 1$  or 2, the heat transfer performance increased with decrease of fin pitch. For  $N \geq 4$  and  $Re_{D_c} > 2000$ , the effect of fin pitch on heat transfer performance was negligible. For the same fin pitch, the effect of the number of tube rows on the friction performance was very small. The effect of tube diameter on heat transfer performance is related to fin pitch as well. Pressure drops for  $D_c = 10.23$  mm exceed those of  $D_c = 8.51$  mm by approximately 10–15%. © 2000 Elsevier Science Ltd. All rights reserved.

*Keywords:* Augmentation; Heat exchangers; Finned surfaces

## 1. Introduction

Plate fin-and-tube heat exchangers of plain fin pattern are employed in a wide variety of engineering applications such as air-conditioning apparatus, process gas heaters and coolers. The fin-and-tube heat exchangers usually consist of mechanically or hydraulically expanded round tubes in a block of parallel continuous fins and, depending on the application, the heat exchangers can be produced with one or more rows. There are many variants regarding fin patterns of plate fin-and-tube heat exchangers, e.g. plain, wavy, louver and convex-louver. Among them, plain fin configura-

tion is still the most popular fin pattern, owing to its simplicity, durability and versatility in application.

During the past few decades, many efforts have been devoted to heat transfer and friction characteristics of plate fin-and-tube heat exchangers. Table 1 summarizes the most influential investigations of the plate fin-and-tube heat exchangers of plain fin geometry since 1971. The most informative studies were those carried out by Rich [1,2], who investigated a total of 14 coils, in which the tube size was 13.34 mm and the longitudinal and transverse tube pitches were 27.5 and 31.75 mm, respectively. He examined the effect of fin spacing and the number of tube rows and concluded that the heat transfer coefficient was essentially independent of the fin spacing and the pressure drop per row is independent of the number of tube rows.

Based on the test results for five heat exchangers (McQuiston, [3],  $F_p = 1.81$ – $6.35$  mm,  $D_o = 9.96$  mm,  $P_1 = 22$  mm,  $P_t = 25.4$  mm and  $N = 4$ ), McQuiston

\* Corresponding author. D500 ERL/ITRI, Bldg. 64, 195–196, Section 4, Chung Hsing Rd., Chutung 310, Hsinchu, Taiwan. Tel.: +886-3-591-6294; fax: +886-3-582-0250.

*E-mail address:* ccwang@itri.org.tw (C.-C. Wang).

Nomenclature			
$A$	area	$R_{eq}$	equivalent radius for circular fin
$A_c$	minimum flow area, $\rho A_{fr}$	$r$	tube inside radius
$A_{fr}$	frontal area	$T$	temperature
$A_o$	total surface area	$\delta_f$	fin thickness
$A_{to}$	external tube surface area	$U$	overall heat transfer coefficient
$C$	heat capacity rate	$V_{fr}$	frontal velocity
$c_p$	specific heat at constant pressure	$V_{max}$	maximum velocity inside the heat exchanger, $V_{max} = V_{fr}/\sigma$ .
$D_c$	fin collar outside diameter, $D_o + 2\delta_f$	$X_L \sqrt{(P_t/2)^2 + P_1^2/2}$	geometric parameter
$D_i$	inside tube diameter	$X_M$	$P_t/2$ , geometric parameter
$D_o$	tube outside diameter	$\delta_w$	thickness of tube wall
$D_h$	hydraulic diameter, $4A_c L/A_o$	$\epsilon$	$\dot{Q}_{ave}/\dot{Q}_{max}$ , heat exchanger effectiveness
$f$	friction factor	$\eta$	fin efficiency
$F_p$	fin pitch	$\eta_o$	surface effectiveness
$G_c$	mass flux of the air based on the minimum flow area, $= \rho V_{max}$	$\mu$	dynamic viscosity of fluid
$h_o$	heat transfer coefficient	$\rho$	density
$j$	$Nu/RePr^{1/3}$ , the Colburn factor	$\sigma$	contraction ratio of cross-sectional area
$k$	thermal conductivity		
$L$	depth of the heat exchanger in airflow direction	<i>Subscripts</i>	
$N$	number of tube rows	1	air side inlet
$\dot{m}$	mass flow rate	2	air side outlet
NTU	$UA/C_{min}$ , number of transfer units	air	air side
$\Delta P$	pressure drop	ave	average value
$P_1$	longitudinal tube pitch	b	base surface
$Pr$	Prandtl number	i	tube side
$P_t$	transverse tube pitch	in	inlet
$\dot{Q}$	heat transfer rate	f	fin surface
$\dot{Q}_{max}$	$C_{min}(T_{water,in} - T_{air,in})$ , the maximum possible heat transfer rate	m	mean value
$r_c$	tube outside radius, including collar thickness	min	minimum value
$Re_{Dc}$	$\rho V D_c / \mu$ , Reynolds number	max	maximum value
		o	total surface
		out	outlet
		water	water side
		w	wall of the tube

[4] proposed the first well known correlation by employing a “finning factor”, defined as  $A_o/A_{to}$ , to correlate his data along with those of Rich [1,2]. His correlation shows a strong dependence of heat transfer performance with the finning factor, i.e.  $j \sim (A_o/A_{to})^{-0.15}$ . For the friction factor correlation, McQuiston [4] claimed the accuracy is  $\pm 35\%$ . Kayansayan [5] also correlated his data (10 samples) using the ‘finning factor’ and showed the  $j$ -factor was proportional to  $(A_o/A_{to})^{-0.362}$ . However, the heat exchangers tested by Kayansayan [5] were all again four-row coil and no frictional data were reported. Furthermore, the experimental data of Kayansayan [5] were con-

siderably lower than those reported by Rich [1,2]. The discrepancies between data of Rich [1,2] and Kayansayan [5] are not clear; however, as pointed out by Wang et al. [6], some of the test data of Kayansayan [5] showed a scattering inconsistency, which may imply some inaccuracies of the test results [5].

Based on the database of five investigations, Gray and Webb [7] proposed an updated correlation for plain fin geometry. It should be mentioned here that the database by Gray and Webb was for  $N \geq 4$  and the database was filtered in advance to prevent “overweighting”. The root-mean-square error of the resulting correlation was 7.3% for heat transfer coefficients

Table 1  
Experimental results for previous investigators<sup>a</sup>

Investigators	Number of samples	$D_o$ (mm)	Fin pitch (mm)	$P_t$ (mm)	$P_1$ (mm)	Row	Test range (m/s)	Correlation
McQuiston and Tree [28]	2	10.3	1.78, 3.18	20.3	17.6	–	0.5–5.9	N
Rich [1]	8	13.3	1.23–8.7	31.8	27.5	4	0.95–21	N
Rich [2]	6	13.2	1.75	31.8	27.5	1–6	1.44–16.3	N
Elmahdy and Biggs [27]	1	9.91	3.14	25.4	22	6	0.8–4.5	Y
	5	13.5	3.81–1.75	31.8	27.4	4		
	1	13.5	2.15	38.1	32.8	8		
McQuiston [3]	5	9.96	1.81–6.35	25.4	22	4	0.5–4	N
McQuiston [4]	–	–	–	–	–	–	–	Y
Kays and London [16]	1	10.21	3.175	25.4	22	–	N	
	1	17.17	3.28	38.1	44.45	–	–	
Gray and Webb [7]	–	–	–	–	–	–	–	Y
Kayansayan [5]	3	9.52	2.34–3.34	25.4	22	4	0.5–10	Y*
	3	9.52	2.34–4.34	30	26	4		
	1	12.5	2.34	31.8	32	4		
	3	16.3	2.34–4.34	40.0	34.7	4		
Seshimo and Fujii [8]	5	6.35	1.2–2.1	20.4	17.7	1–2	0.5–2.5	Y*
	8	7.94	1.2–2.3	20.4	17.7	1		
	4	9.52	1.5	25.4	32/22/20/18	1		
		9.52	25.4	20.4	17.7			
	4	9.52	1.0–6.0	25.4	22	1–5		
Wang et al. [6]	15	10.06	1.74–3.2	25.4	22	2–6	0.3–6.5	Y
Wang et al. [9]	4	7.2	1.21, 1.71	20.4	12.7	2–3	0.3–8.0	Y*
Present investigation	18	7.3	1.21–1.78	21	12.7	2, 4	0.3–6.5	Y
		8.28	1.21–2.06	25.4	19.05	1–4		
		10.0	1.21–2.06	25.4	19.05	1–4		

<sup>a</sup> The test samples are all staggered layout. The correlation developed by Seshimo and Fujii [8] is valid for 1 and 2 row. The correlation proposed by Kayansayan [5] is only for heat transfer data. The correlation proposed for Wang et al. [7] is a modification of Gray and Webb correlation and the modification is only for heat transfer data.

and 7.8% for friction factors. Notice that the Gray and Webb [7] correlation gave reasonably predictive ability for those having larger tube diameter, larger longitudinal tube pitch and transverse tube pitch. A significant improvement of the Gray and Webb [7] correlation is their friction factor correlation, which is superior to McQuiston's [4] correlation. Seshimo and Fujii [8] provided test results for a total of 35 samples, but their test range was limited to  $0.5 \text{ m}\cdot\text{s}^{-1} < V_{fr} < 2.5 \text{ m}\cdot\text{s}^{-1}$ . Recently, Wang et al. [6] reported airside performance for 15 samples of plain fin-and-tube heat exchangers. They examined effects of several geometrical parameters, including the number of tube rows, fin spacing and fin thickness. Their test samples were limited to  $D_c = 10.3 \text{ mm}$ ,  $P_1 = 22 \text{ mm}$ ,  $P_t = 25.4 \text{ mm}$  and  $N = 2-6$ . Wang et al. [6] argued that the occurrence of "maximum phenomenon" for the Colburn  $j$  factors at a large number of tube rows and small fin spacing may not be associated with the experimental uncertainties,

as commented by Rich<sup>1</sup>. They also proposed a heat transfer and friction correlation to describe their own data set ( $P_1 = 22 \text{ mm}$  and  $P_t = 25.4 \text{ mm}$ ).

Though numerous studies had been devoted to plain fin-and-tube heat exchangers, however, most of the previously published data were for large tube diameter (e.g.  $D_o = 9.52, 12.7$  and  $15.8 \text{ mm}$ ). In modern applications of air-cooled heat exchangers, the tube size is generally less than 10 mm and the corresponding longitudinal and transverse tube pitches are getting smaller and smaller. Recently, the use of even smaller tubes (like 7.94- and 7-mm tubes) in residential application is becoming popular. This is because possible higher heat transfer coefficients, lower pressure drops and less refrigerant charge can be achieved by using smaller tubes, and can eventually lead to much more compact fin-and-tube heat exchanger design. This is especially helpful in space-limited areas. In a recent investigation, based on the test results of four plain fin-and-tube exchangers with  $D_c = 7.59 \text{ mm}$ ,  $P_t = 21 \text{ mm}$ ,  $P_1 = 12.7 \text{ mm}$  and  $N = 2-3$ , Wang et al. [9] reported that the Gray and Webb correlation may significantly underpredict the heat transfer performance.

<sup>1</sup> D.G. Rich, private discussion with Prof. Webb, 1986, quoted in Gray and Webb [7] paper.

In this connection, the present authors feel that further experimental information is needed (especially about those having smaller  $D_c$ ,  $P_t$  and  $P_l$ ). Thus, the objective of the present study is to provide new experimental data for the plain fin-and-tube heat exchangers having  $D_o=9.52$ , 7.94, and 7 mm (before expansion).

## 2. Experimental apparatus

The sample coils are all plain fin configuration. Their detailed geometric parameters are tabulated in Table 2. Detailed construction of the circuitry arrangement is identical to those by Seshimo and Fujii [8] and Wang et al. [10]. All tests were conducted in an open wind tunnel as shown in Fig. 1. The ambient air flow was forced across the test section by means of a 5.6-kW centrifugal fan with an inverter. To avoid and minimize the effect of flow maldistribution in the experiments, an air straightener–equalizer and a mixer were provided. The inlet and the exit temperatures across the sample coil were measured by two T-type thermocouple meshes. The inlet measuring mesh consists of 12 thermocouples, while the outlet mesh contains 36 thermocouples. The sensor locations inside the rectangular duct were established following ASHRAE [11] recommendations. These data signals were individually recorded and then averaged. During the isothermal test, the variance of these thermocouples was within  $\pm 0.2^\circ\text{C}$ . In addition, all the thermocouples were

precalibrated by a quartz thermometer with  $0.01^\circ\text{C}$  precision.

The pressure drop of the test coil was detected by a precision differential pressure transducer, reading to 0.1 Pa. The air flow measuring station was a multiple nozzle code tester based on the ASHRAE 41.2 standard [12]. The working medium in the tube side was hot water. The inlet water temperature was controlled by a thermostat reservoir having an adjustable capacity up to 60 kW. Both the inlet and outlet temperatures were measured by two precalibrated RTDs (resistance temperature device, Pt—100  $\Omega$ ). Their accuracy was within  $0.05^\circ\text{C}$ . The water volumetric flow rate is detected by a magnetic flow meter with 0.002 l/s resolution.

All the data signals are collected and converted by a data acquisition system (a hybrid recorder). The data acquisition system then transmitted the converted signals through a GPIB interface to the host computer for further operation. During the experiments, the water inlet temperature was held constant at  $65.0 \pm 0.2^\circ\text{C}$  and the tube side Reynolds number was approximately 38,000. Frontal velocities ranged from 0.3 to 6.5 m/s. The energy un-balance between air side and tube side was within 3%. The water side resistance (evaluated as  $1/h_i A_i$ ) was less than 15% of the overall resistance in all cases. The test fin-and-tube heat exchangers are tension-wrapped, having a “L” type fin collar. Thermal contact conductance provided by the manufacturers ranged from 11,000 to 16,000  $\text{W}\cdot\text{m}^{-2}\cdot\text{K}$ . Uncertainties in the reported experimental values of

Table 2  
Geometric dimensions of the sample plate fin-and-tube heat exchangers<sup>a</sup>

No.	Nominal tube diameter (mm)	$D_c$ (mm)	Fin pitch (mm)	$P_t$ (mm)	$P_l$ (mm)	Number of tube rows
1	7	7.53	1.22	21	12.7	2
2	7	7.53	1.78	21	12.7	2
3	7	7.53	1.22	21	12.7	4
4	7	7.53	1.78	21	12.7	4
5	7.94	8.51	1.19	25.4	19.05	1
6	7.94	8.51	2.04	25.4	19.05	1
7	7.94	8.51	1.23	25.4	19.05	2
8	7.94	8.51	2.06	25.4	19.05	2
9	7.94	8.51	1.23	25.4	19.05	4
10	7.94	8.51	1.60	25.4	19.05	4
11	7.94	8.51	2.06	25.4	19.05	4
12	9.52	10.23	1.23	25.4	19.05	1
13	9.52	10.23	2.23	25.4	19.05	1
14	9.52	10.23	1.23	25.4	19.05	2
15	9.52	10.23	2.23	25.4	19.05	2
16	9.52	10.23	1.23	25.4	19.05	4
17	9.52	10.23	1.55	25.4	19.05	4
18	9.52	10.23	2.31	25.4	19.05	4

<sup>a</sup> The test samples are all staggered layout. Fin thickness of all the test samples are 0.115 mm.

the Colburn  $j$  factor and friction factor  $f$  were estimated by the method suggested by Moffat [13]. The uncertainties ranged from 3.2 to 15.9% for the  $j$  factor and 3.3 to 22.3% for  $f$ . The highest uncertainties were associated with lowest Reynolds number.

### 3. Analysis

To obtain the heat transfer and pressure loss characteristics of the test coil from the experimental data, the  $\epsilon$ -NTU method is applied to determine the UA product in the analysis. The total heat transfer rate used in the calculation is the mathematical average of the air side and the water side heat transfer rates, namely,

$$\dot{Q}_{\text{air}} = \dot{m}_{\text{air}} c_{p,\text{air}} \Delta T_{\text{air}} \quad (1)$$

$$\dot{Q}_{\text{water}} = \dot{m}_{\text{water}} c_{p,\text{water}} \Delta T_{\text{water}} \quad (2)$$

$$\dot{Q}_{\text{ave}} = (\dot{Q}_{\text{water}} + \dot{Q}_{\text{air}})/2 \quad (3)$$

In the  $\epsilon$ -NTU method, the number of heat transfer units (NTU) is defined as

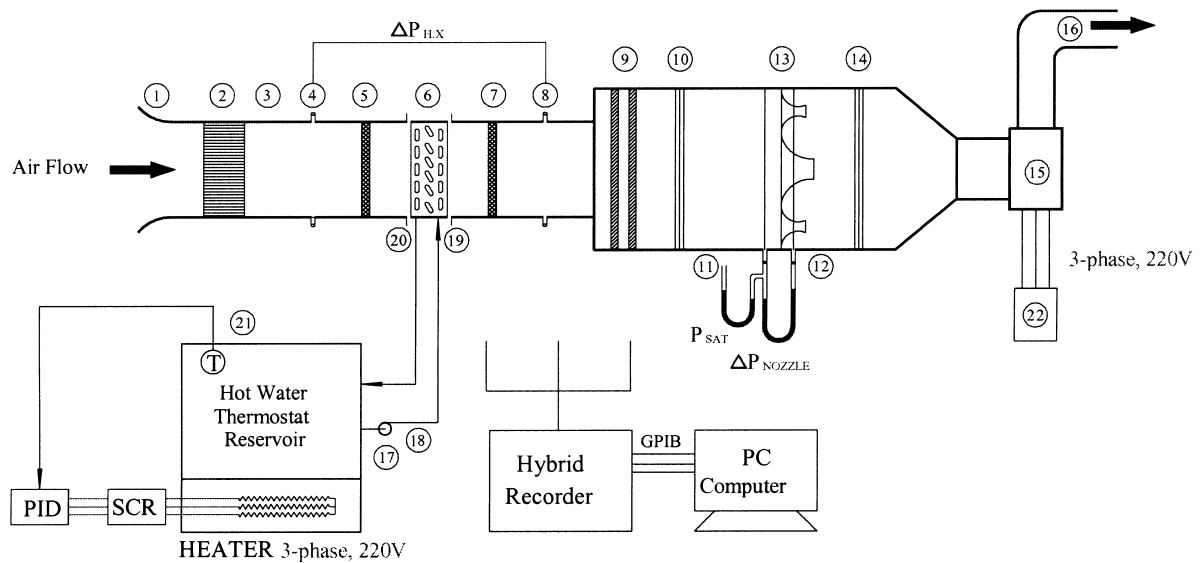
$$\text{NTU} \equiv UA/C_{\text{min}} \quad (4)$$

The UA product was calculated using the  $\epsilon$ -NTU relationship accounting the effect of the number of tube rows from ESDU [14] and is depicted in Table 3. Definitions of  $C^*$  and  $\epsilon$  are given as follows:

$$C^* \equiv \frac{C_{\text{min}}}{C_{\text{max}}} = \frac{\dot{m}_{\text{air}} c_{p,\text{air}}}{\dot{m}_{\text{water}} c_{p,\text{water}}} \quad (6)$$

$$\epsilon \equiv \frac{\dot{Q}_{\text{ave}}}{\dot{Q}_{\text{max}}} = \frac{\dot{Q}_{\text{ave}}}{C_{\text{min}}(T_{\text{in,water}} - T_{\text{in,air}})} \quad (7)$$

The overall heat transfer resistance is defined from the following relationship,



- |  |   |
|--|---|
| 1 Air inlet                                | 12 Nozzle pressure tap(outlet)          |
| 2 Straightener                             | 13 Multiple nozzles plate               |
| 3 Developing section                       | 14 Settling Devices (Flow Straightener) |
| 4 Pressure tap(inlet)                      | 15 Centrifugal fan                      |
| 5 T/C inlet temperature measuring station  | 16 Air discharge                        |
| 6 Test unit(Heat Exchanger)                | 17 Water pump                           |
| 7 T/C outlet temperature measuring station | 18 Water flow meter                     |
| 8 Pressure tap(outlet)                     | 19 RTD inlet temperature of water side  |
| 9 Mixer                                    | 20 RTD outlet temperature of water side |
| 10 Settling Devices (Flow Straightener)    | 21 Temperature sensor                   |
| 11 Nozzle pressure tap(inlet)              | 22 Inverter                             |

Fig. 1. Schematic of test facility.

$$\frac{1}{UA} = \frac{1}{\eta_o h_o A_o} + \frac{1}{2} \log_e \left( \frac{D_o}{D_i} \right) \frac{D_o}{k_w A_w} + \frac{1}{h_i A_i} \quad (8)$$

The tube-side heat transfer coefficient,  $h_i$ , is evaluated from the Gnielinski [15] semi-empirical correlation

$$h_i = \left( \frac{k}{D} \right)_i \frac{(Re_i - 1000) Pr (f_i/2)}{1 + 12.7 \sqrt{f_i/2} (Pr^{2/3} - 1)} \quad (9)$$

where

$$f_i = (1.58 \ln(Re_{D_i}) - 3.28)^{-2} \quad (10)$$

where  $Re_{D_i} = \rho V D_i / \mu$ . The surface efficiency,  $\eta_o$ , is defined as the actual heat transfer for the fin and base divided by the heat transfer for the fin and base when the fin is at the same base temperature  $T_b$ . This term may be written in terms of the fin efficiency  $\eta$ , fin surface area  $A_f$  and total surface area  $A_o$ , i.e.

$$\eta_o = 1 - \frac{A_f}{A_o} (1 - \eta) \quad (11)$$

where  $A_o = A_f + A_b$  and  $A_f$ ,  $A_b$  are the areas of the fin and base, respectively.  $\eta$  denotes fin efficiency and is calculated by the approximation method described by Schmidt [16].

$$\eta = \frac{\tanh(mr\phi)}{mr\phi} \quad (12)$$

where

$$m = \sqrt{\frac{2h_o}{k_f \delta_f}} \quad (13)$$

$$\phi = \left( \frac{R_{eq}}{r} - 1 \right) [1 + 0.35 \ln(R_{eq}/r)] \quad (14)$$

$$\frac{R_{eq}}{r} = 1.27 \frac{X_M}{r} \left( \frac{X_L}{X_M} - 0.3 \right)^{1/2} \quad (15)$$

With Eqs. (12)–(15), an iterative procedure is needed

Table 3  
 $\epsilon$ -NTU relationship for cross-flow configuration<sup>a</sup>

Number of tube rows	Side of $C_{min}$	Formula
1	air	$\epsilon = [1 - e^{-C^*(1-e^{-NTU})}] / C^*$
	tube	$\epsilon = 1 - e^{-((1-e^{-NTU \cdot C^*})/C^*)}$
2	air	$\epsilon = [1 - e^{-2KC^*} (1 + C^* K^2)] / C^*, K = 1 - e^{-NTU/2}$
	tube	$\epsilon = 1 - e^{-2K/C^*} (1 + (K^2/C^*)), K = 1 - e^{-NTU \cdot C^*/2}$
3	air	$\epsilon = [1 - e^{-3KC^*} (1 + C^* K^2 (3 - K) + (3(C^*)^2 K^4/2))] / C^*, K = 1 - e^{-NTU/3}$
	tube	$\epsilon = 1 - e^{-3K/C^*} (1 + (K^2(3 - K)/C^*) + (3K^4/2(C^*)^2)) / K = 1 - e^{-NTU \cdot C^*/3}$
4	air	$\epsilon = [1 - e^{-4KC^*} (1 + C^* K^2 (6 - 4K + K^2) + 4(C^*)^2 K^4 (2 - K) + (8(C^*)^3 K^6/3))] / C^*,$ $K = 1 - e^{-NTU/4}$
	tube	$\epsilon = 1 - e^{-4K/C^*} (1 + (K^2(6 - 4K + K^2)/C^*) + (4K^4(2 - K)/(C^*)^2) + (8K^6/3(C^*)^3)),$ $K = 1 - e^{-NTU \cdot C^*/4}$
$\infty$	–	$\epsilon = 1 - \exp[NTU^{0.22} \cdot \{\exp(-C^* \cdot NTU^{0.78}) - 1\} / C^*]$

<sup>a</sup> Unmixed–unmixed formula.

to obtain the airside heat transfer coefficient  $h_o$  and the surface efficiency  $\eta_o$ . The airside heat transfer characteristics are presented in terms of the Colburn  $j$  factor:

$$j = \frac{h_o}{\rho V_{\max} C p_a} P r^{2/3} \quad (16)$$

where  $V_{\max} = V_{fr}/\sigma$ . The term,  $\sigma$ , is the ratio of the minimum flow area to frontal area. All the fluid properties are evaluated at the average values of the inlet and outlet temperatures under the steady state condition. The friction factors are calculated from the pressure drop equation proposed by Kays and London [17]. The relation for the nondimensional friction factor,  $f$ , in terms of pressure drop is shown below:

$$f = \frac{A_c}{A_o} \frac{\rho_m}{\rho_1} \left[ \frac{2\Delta P \rho_1}{G_c^2} - (1 + \sigma^2) \left( \frac{\rho_1}{\rho_2} - 1 \right) \right] \quad (17)$$

where  $A_o$  and  $A_c$  stand for the total surface area and the flow cross-sectional area, respectively.

#### 4. Results and discussion

Fig. 2 depicts the effect of fin pitch on the heat transfer and friction characteristics having 4-row configuration. As is seen in the figure, the heat transfer

performance is independent of fin pitch for both types of configuration ( $D_c = 10.23$  and  $D_c = 7.52$  mm). Regarding the effect of fin pitch on heat transfer performance, Rich [1] concluded that the heat transfer coefficients were essentially independent of fin spacing having 4-row configuration. The experimental data of Wang et al. [6] also supported this result for plain fin-and-tube heat exchangers having 4-row configuration. Analogous to the test results of plain fin pattern, Wang et al. [18–22] also conclude that the effect of fin pitch on the heat transfer performances is also negligible for multirow louver and wavy fin geometry.

However, for the heat transfer performance of 1- and 2-row configuration, as illustrated in Fig. 3, the heat transfer performance shows detectable dependence on the fin pitch. For  $Re_{D_c} > 5000$ , the effect of fin pitch is negligible. The results can be explained by the interpretations of previous investigations [23,24]. Based on the naphthalene sublimating method, Saboya and Sparrow [23] indicated that boundary development is the most important factor for the 1-row coil and the effect of vortex may gain in importance at higher Reynolds number. Therefore, as shown in the present test results, the effect of fin pitch diminished for  $Re_{D_c} > 5000$ . For  $Re_{D_c} < 5000$ , the heat transfer performance increases with decrease of fin pitch. This phenomenon is seen for  $N \geq 2$  and is especially pronounced for  $N = 1$ . The phenomenon can be further

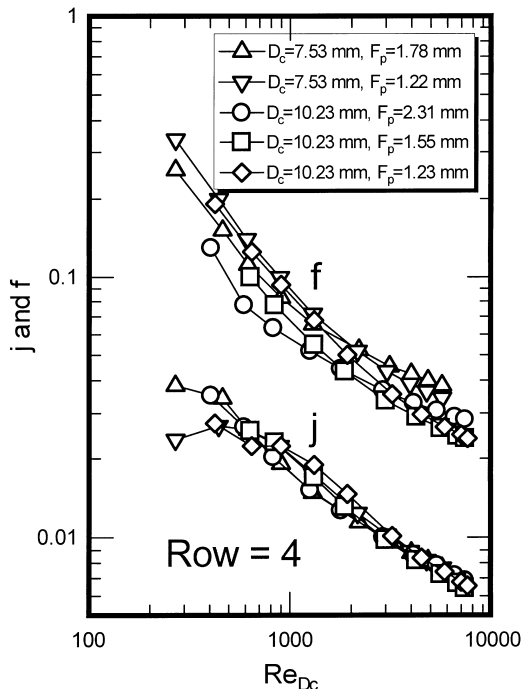


Fig. 2. Effect of fin pitch on heat transfer and friction characteristics having  $N = 4$ .

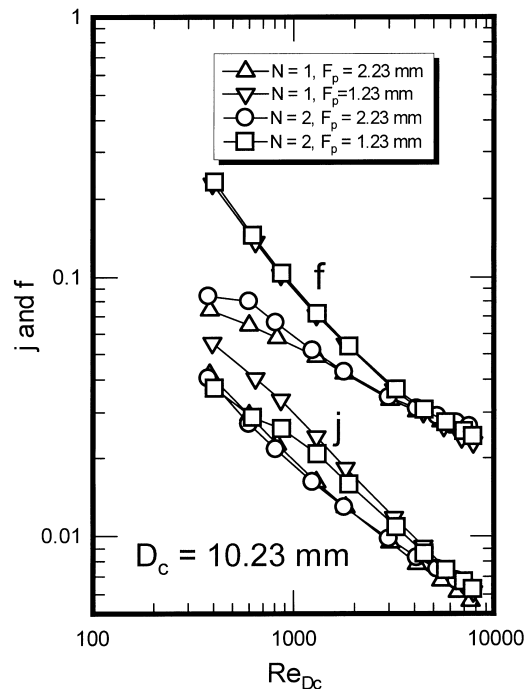


Fig. 3. Effect of fin pitch on heat transfer and friction characteristics having  $N = 1$  and  $N = 2$ .

explained from the numerical results of the effect of fin pitch carried out by Torikoshi et al. [24]. They conducted a 3D numerical investigation of a 1-row plain fin-and-tube heat exchanger. A schematic of their results is plotted in Fig. 4a and b. Their investigation shows that the vortex that forms behind the tube can be suppressed and the entire flow region can be kept steady and laminar when the fin pitch is small enough (e.g.  $F_p/D = 0.17$ , Fig. 4a). Further increase of  $F_p/D$  to 0.3 would result in a noticeable increase of the cross-stream width of the vortex region behind the tube (Fig. 4b). As a result, lower heat transfer performance is seen for larger  $F_p/D$  for 1-row configuration. For the numerical results of 2-row configuration by Torikoshi and Xi [25], the first row cylinder is stabilized due to the existence of the second tube row, rather than in the wake of the first row as seen in Fig. 4c. Therefore, the 2-row coil still reveals similar results as those of 1-row coils. However, it can be seen that the effect of fin pitch for  $N = 2$  becomes less profound in comparison with  $N = 1$ .

With further increase of the number of tube rows ( $N \geq 4$ ), the airflow within the heat exchanger may become periodic and results in the “vortex-controlled” regime. Consequently, the effect of fin pitch on heat transfer performance vanishes for  $N = 4$ . This phenomenon can be further substantiated from the test results of friction factors. In comparison with the test results of the 4-row coil (vortex dominated) in Fig. 2, the closing of friction factors vs. the Reynolds number is apparently lower ( $Re_{D_c} \approx 2000\text{--}3000$ ). Xi [26] also

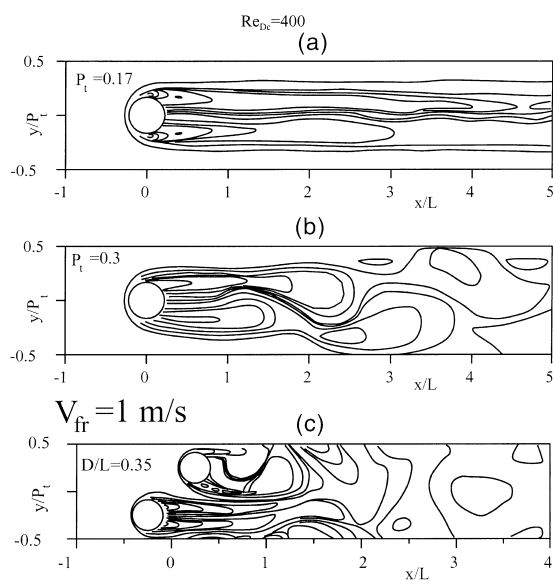


Fig. 4. Schematic illustration of 3D computational results for the effect of fin pitch (taken from those by Torikoshi et al. [24] and Torikoshi and Xi [25]).

showed that higher velocity and larger number of tube rows may result in the occurrence of vortex along the fins, therefore the effect of fin pitch on heat transfer coefficient would be negligible.

Fig. 5 illustrates the effect of the number of tube rows on the heat transfer and friction characteristics. The number of tube rows are 1, 2 and 4, respectively. The fin pitch is approximate 1.2 mm. As can be seen, the Colburn  $j$  factors decrease with increase of the number of tube rows for  $Re_{D_c} < 3000$ . However, the effect of the number of tube rows diminishes as the Reynolds number increase over 3000. This phenomenon is very similar to the test results reported by Rich [2] and Wang et al. [6]. At a higher Reynolds region, the airflow and temperature distribution inside of heat exchanger may easily become unsteady due to vortex formation and shedding. Hence, higher heat transfer performance is seen and eventually the effect of the number of tube rows on heat transfer coefficient becomes negligible. As the Reynolds number is decreased, the effect of downstream turbulence tends to diminish. As a result, significant degradation of the heat transfer performance is observed for  $Re_{D_c} < 3000$ . Xi [26] also pointed out that in the case of lower Reynolds number, flow and thermal fields inside of heat exchanger are laminar. Therefore, at any fin pitches, the heat transfer coefficient decreases as the row number increases. Furthermore, the decreasing tendency of

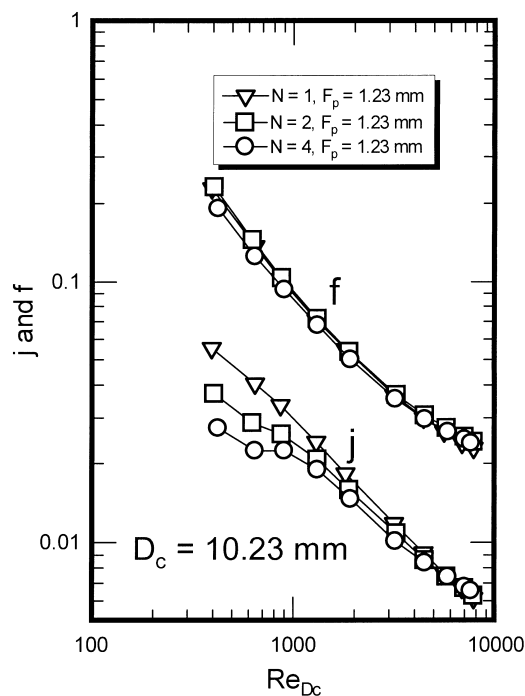


Fig. 5. Effect of the number of tube rows on the heat transfer and friction characteristics ( $F_p = 1.23$  mm).



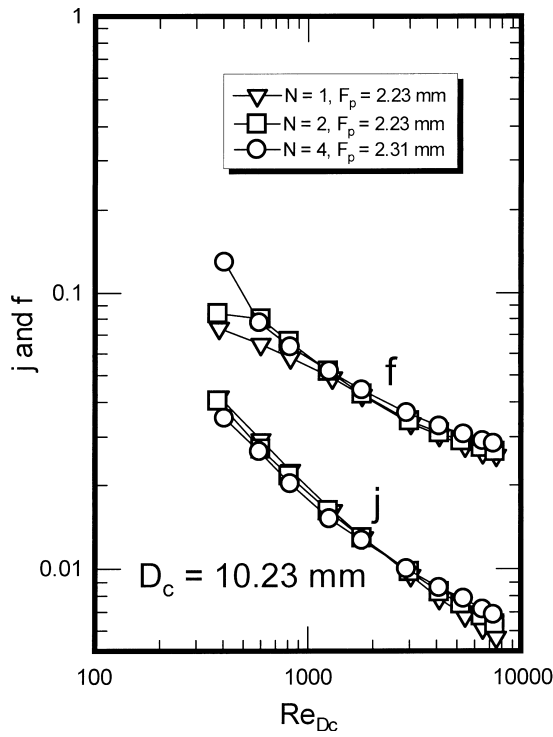


Fig. 6. Effect of the number of tube rows on the heat transfer and friction characteristics ( $F_p = 2.23\text{--}2.31\text{ mm}$ ).

heat transfer coefficient vs. the number of tube rows is different when fin pitch is increased. In the case of larger fin pitch ( $F_p \approx 2.2\text{ mm}$ ) shown in Fig. 6, one can clearly see that the effect of the number of tube rows on the heat transfer performance at low Reynolds numbers, is almost negligible. Figs. 5 and 6 also indicate that for multiple-row coils, the friction factors are independent of the number of tube rows.

The effect of tube diameter on the heat transfer and friction characteristics for 1-row and 2-row is shown in Fig. 7 ( $F_p \approx 1.2\text{ mm}$ ). As seen, the heat transfer coefficients for  $D_c = 8.51\text{ mm}$  are slightly higher than those of  $D_c = 10.23\text{ mm}$  for  $N = 2$ . In addition, the pressure drops for  $D_c = 10.23$  are 10–15% higher than those of  $D_c = 8.51\text{ mm}$ . The results agree with the 3D numerical simulation carried out by Torikoshi and Xi [24]. The larger diameter tube may increase the ineffective area behind the tubes. However, for  $N = 1$ , the heat transfer coefficients for  $D_c = 10.23\text{ mm}$  are slightly higher than those of  $D_c = 8.51\text{ mm}$ . A possible explanation may be due to the ineffective area of the 1-row configuration is comparatively small.

For a larger fin pitch near 2.2 mm, analogous results are seen in Fig. 8. Notice that the fin pitch for  $D_c = 8.51$  is about 4–5% lower than that of  $D_c = 10.23\text{ mm}$ . Hence, a slight difference in heat transfer performance is seen for  $V_{fr} < 1.5\text{ m}\cdot\text{s}^{-1}$ . The effect of tube diameter on the heat transfer perform-

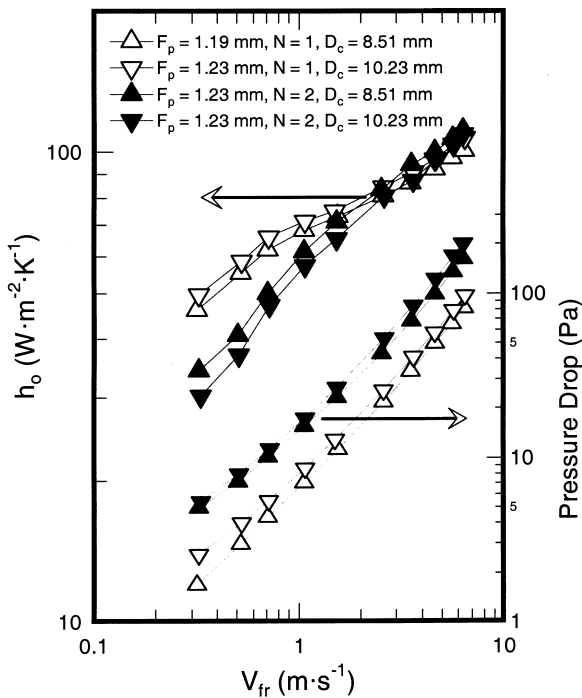


Fig. 7. Effect of the tube diameter row on the heat transfer and friction characteristics ( $F_p = 1.21\text{ mm}$ ,  $N = 1$  and 2).

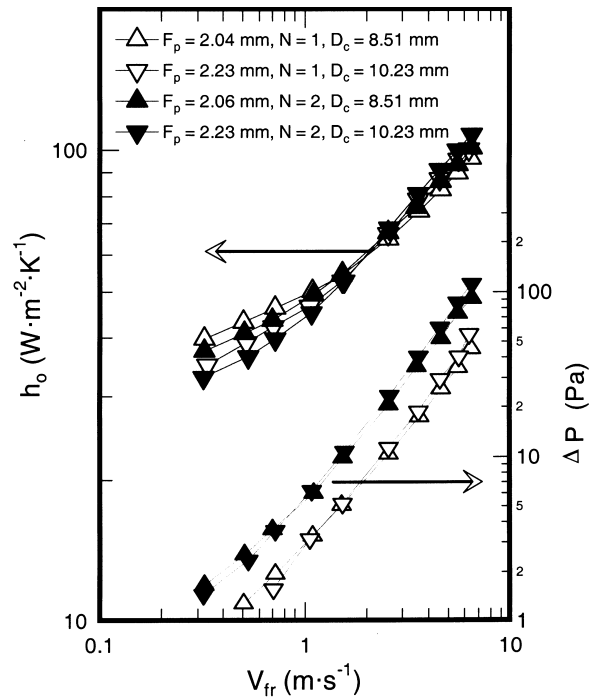


Fig. 8. Effect of the tube diameter row on the heat transfer and friction characteristics ( $F_p = 2.04\text{--}2.23\text{ mm}$ ,  $N = 1$  and 2).

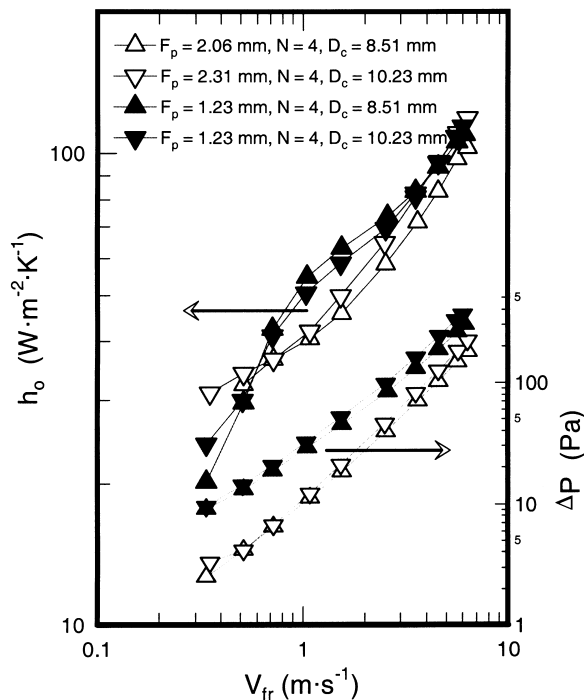


Fig. 9. Effect of the tube diameter row on the heat transfer and friction characteristics ( $N = 4$ ,  $F_p = 1.21$ – $2.23$  mm).

ance is almost reversed when compared with those of  $F_p \approx 1.2$  mm and  $N = 4$  (Fig. 9). Basically, the heat transfer performance for  $D_c = 10.23$  mm is higher than those of  $D_c = 8.51$  mm, except at very low frontal velocity. The characteristics of the pressure drops are similar to those of  $F_p \approx 1.2$  mm.

## 5. Conclusions

On the basis of previous discussions, the following conclusions are made:

- The effect of fin pitch on the Colburn  $j$  factors is negligible for  $N \geq 4$  and  $Re_{D_c} > 2000$  owing to the effect of vortex formation along the fin. The present test data indicate that the heat transfer coefficients increase with decrease fin pitch for  $300 < Re_{D_c} < 3000$  and  $N = 1, 2$ .
- The effect of tube row on the heat transfer performance is especially pronounced at low Reynolds number where the number of tube rows is large and the fin pitch is small. The effect of the number of tube rows on friction performance is comparatively small.
- For  $F_p \approx 1.2$  mm, the effect of tube diameter on the heat transfer coefficients is rather small. However, the pressure drops for  $D_c = 10.23$  mm are 5–15% higher than those of  $D_c = 8.51$  mm. Similar results were observed for  $F_p \approx 2.2$  mm.

## Acknowledgements

The authors would like to express gratitude for financial support from the Energy R&D foundation of the Energy Commission of the Ministry of Economic Affairs, Taiwan.

## References

- [1] D.G. Rich, The effect of fin spacing on the heat transfer and friction performance of multirow, smooth plate fin-and-tube heat exchangers, ASHRAE Trans. 79 (2) (1973) 135–145.
- [2] D.G. Rich, The effect of the number of tubes rows on heat transfer performance of smooth plate fin-and-tube heat exchangers, ASHRAE Trans. 81 (1) (1975) 307–317.
- [3] F.C. McQuiston, Heat, mass and momentum transfer data for five plate-fin-tube heat transfer surfaces, ASHRAE Trans. 84 (1) (1978) 266–293.
- [4] F.C. McQuiston, Correlation of heat, mass and momentum transport coefficients for plate-fin-tube heat transfer surface, ASHRAE Trans. 84 (1) (1978) 294–308.
- [5] N. Kayansayan, Heat transfer characterization of flat plain fins and round tube heat exchangers, Exp. Therm. Fluid Sci. 6 (1993) 263–272.
- [6] C.C. Wang, Y.C. Hsieh, Y.J. Chang, Y.T. Lin, Sensible heat and friction characteristics of plate fin-and-tube heat exchangers having plane fins, Int. J. Refrig. 19 (4) (1996) 223–230.
- [7] D.L. Gray, R.L. Webb, Heat transfer and friction correlations for plate finned-tube heat exchangers having plain fins, in: Proc. 8th Heat Transfer Conference, 1986, pp. 2745–2750.
- [8] Y. Seshimo, M. Fujii, An experimental study of the performance of plate fin and tube heat exchangers at low Reynolds number, in: Proceeding of the 3rd ASME/JSME Thermal Engineering Joint Conference, vol. 4, 1991, pp. 449–454.
- [9] C.C. Wang, W.S. Lee, C.T. Chang, Sensible heat transfer characteristics of plate fin-and-tube exchangers having 7-mm tubes, AIChE Symp. Ser. 93 (314) (1997) 211–216.
- [10] C.C. Wang, C.J. Lee, C.T. Chang, S.P. Lin, Heat transfer and friction correlation for compact louvered fin-and-tube heat exchangers, Int. J. Heat Mass Transfer 12 (12) (1999) 1945–1956.
- [11] ASHRAE, in: Handbook Fundamental, SI-Edition, American Society of Heating, Refrigerating and Air-Conditioning Engineers, Atlanta, 1993, pp. 14–15 (ch. 13).
- [12] ASHRAE Standard 41.2, 1987, Standard Methods for Laboratory Air-flow Measurement, American Society of Heating, Refrigerating and Air-Conditioning Engineers, Atlanta, 1987.
- [13] R.J. Moffat, Describing the uncertainties in experimental results, Exp. Therm. Fluid Sci. 1 (1988) 3–17.
- [14] ESDU 86018, in: Engineering Science Data Unit 86018

- with Amendment A, ESDU International plc, London, 1991, pp. 92–107.
- [15] V. Gnielinsk, New equation for heat and mass transfer in turbulent pipe and channel flow, *Int. Chem. Eng.* 16 (1976) 359–368.
- [16] Th.E. Schmidt, Heat transfer calculations for extended surfaces, *Refrigerating Engineering*, April (1949) 351–357.
- [17] W.M. Kays, A.L. London, *Compact Heat Exchangers*, 3rd ed., McGraw-Hill, New York, 1984.
- [18] C.C. Wang, Y.P. Chang, K.U. Chi, Y.J. Chang, An experimental study of heat transfer and friction characteristics of typical louver fin and tube heat exchangers, *Int. J. Heat Mass Transfer* 41 (4–5) (1998) 817–822.
- [19] C.C. Wang, Y.P. Chang, K.U. Chi, Y.J. Chang, A study of nonredirection louver fin-and-tube heat exchangers. *Proceeding of Institute of Mechanical Engineering, Part C, Journal of Mechanical Engineering Science*, 212 (1998) 1–14.
- [20] C.C. Wang, C.J. Lee, C.T. Chang, Some aspects of the fin-and-tube heat exchangers: with and without Louvers, *J. Enhanc. Heat Transfer* 6 (1999) 357–368.
- [21] C.C. Wang, W.L. Fu, C.T. Chang, Heat transfer and friction characteristics of typical wavy fin-and-tube heat exchangers, *Exp. Therm. Fluid Sci.* 14 (2) (1997) 174–186.
- [22] C.C. Wang, Y.M. Tsi, D.C. Lu, Comprehensive study of convex-louver and wavy fin-and-tube heat exchangers, *AIAA J. Thermophys. Heat Transfer* 12 (3) (1998) 423–430.
- [23] E.M. Saboya, E.M. Sparrow, Transfer characteristics of two-row plate fin and tube heat exchanger configurations, *Int. J. Heat Mass Transfer*, 19, pp. 41–49.
- [24] K. Torikoshi, G. Xi, Y. Nakazawa, H. Asano, Flow and heat transfer performance of a plate-fin and tube heat exchanger (1st report: effect of fin pitch), in: 10th *Int. Heat Transfer Conf.* 1994, paper 9-HE-16, 1994, pp. 411–416.
- [25] K. Torokoshi, G. Xi, A numerical study of flow and thermal fields in finned tube heat exchangers (effect of the tube diameter), *ASME HTD* 317 (1) (1995) 453–458.
- [26] G.N. Xi, 1997, Private communication.
- [27] P.E. Elmahdy, P.E. Briggs, Finned tube heat exchangers: correlation of dry surface data, *ASHRAE Trans.* 85 (2) (1979) 262–273.
- [28] F.C. McQuiston, D.R. Tree, heat transfer and flow friction data for two fin-tube surfaces, *ASME J. Heat Transfer* 93 (1971) 249–250.